Journal of Molecular Spectroscopy 348 (2018) 117–123

Contents lists available at ScienceDirect

Journal of Molecular Spectroscopy

journal homepage: www.elsevier.com/locate/jms

# Infrared spectroscopy of isoprene in noble gas matrices

Fumiyuki Ito

*National Institute of Advanced Industrial Science and Technology (AIST), Tsukuba West, Onogawa 16-1, Tsukuba, Ibaraki 305-8569, Japan*

ARTICLE INFO

*Article history:*
Received 4 November 2016
In revised form 20 January 2017
Accepted 13 February 2017
Available online 16 February 2017

*Keywords:*
Isoprene
Matrix isolation
Infrared spectroscopy
Density functional theory
Anharmonic vibrational calculation

ABSTRACT

In this study, the infrared absorption spectra of 2-methyl-1,3-butadiene (isoprene) in noble gas matrices (Ar, Kr, and Xe) have been reported. The vibrational structure observed at cryogenic temperature, in combination with anharmonic vibrational calculations using density functional theory, helped in unambiguously assigning the fundamental modes of isoprene unresolved in the previous gas phase measurements, which would be of basic importance in the remote sensing of this molecule. A careful comparison with the most recent gas phase study [Brauer et al., Atmos. Meas. Tech. 7 (2014) 3839–3847.] led us to alternative assignments of the weak bands.

© 2017 Elsevier Inc. All rights reserved.

## 1. Introduction

Isoprene (2-methyl-1,3-butadiene) accounts for approximately one-third of the annual global emissions of volatile organic compounds (VOCs) from all natural and anthropogenic sources in the troposphere [1]. It reacts with ozone to produce carbonyl products and a Criegee intermediate via a primary ozonide, which contributes to secondary organic aerosol formation [2]. Thus, it is essential to detect isoprene *in situ* by spectroscopic techniques [3].

In this regard, spectroscopic studies of isoprene have been conducted in the microwave [4] and infrared (IR) regions [5–11]. A weak absorption of this molecule in the UV region has also been measured using cavity ringdown spectroscopy [12]. The preceding IR studies involve gas-phase measurements with moderate spectral resolution at room temperature; however, the assignment of fundamental bands is complicated because of the overlap of rotational contours. Panchenko et al. have conducted a series of theoretical studies of isoprene by *ab initio* methods for clarifying its complex band structures [6–9,11]. Recently Brauer et al. observed well-resolved band profiles and successfully determined center frequency and band intensity for each fundamental band [10]. Nevertheless, the assignment in the C—H bending (7 μm) and C—H stretching (3.3 μm) regions still remains unresolved. Although spectroscopic measurements at low temperatures—either under jet-cooled conditions or using cold matrices—may improve this situation, such measurements have not been reported thus far, to the best of our knowledge.

Hence, this study aims to provide the first report on the spectroscopic data for isoprene at cryogenic temperatures by matrix isolation technique. The IR spectra measured in noble gas matrices (Ar, Kr, and Xe) are compared with anharmonic vibrational frequencies obtained from the second-order vibrational perturbation theory (VPT2) [13] for assigning vibrational peaks, as has been reported previously [14]. Special care was taken to compare the present results with the most recent gas phase work [10], in order to obtain consistency in the vibrational assignments.

## 2. Experimental

Isoprene was purchased from Wako Pure Chemical Industry (Osaka, Japan) and used after degassing via freeze–pump–thaw cycles. Premixed samples of isoprene were prepared by mixing the vapor and noble gas at various ratios in a stainless steel vessel. Each gaseous sample was deposited on a cold CsI surface maintained at cryogenic temperature. Typically, the substrate was maintained at 20 K for Ar, 35 K for Kr, and 45 K for Xe. Other experimental and instrumental details have been described elsewhere [14–20]. For comparison, a gas-phase IR spectrum of isoprene was also measured in a White-type multipath cell using a JASCO FT/IR-620 spectrometer with a resolution of 0.25 $cm^{-1}$.

Fig. 1 shows the spectrum of isoprene in the Ar matrix, with the vibrational assignments based on the Herzberg notation [21]. The two insets show well-resolved vibrational peaks in the C—H bending and C—H stretching regions, respectively, which are obscured in the gas-phase spectrum at ambient temperature. Instrumental limitations did not allow us to locate vibrational peaks below 800 $cm^{-1}$. Fig. 2 shows the comparison of the IR spectra in Ar, Kr,

*E-mail address:* f-ito@aist.go.jp

http://dx.doi.org/10.1016/j.jms.2017.02.010
0022-2852/© 2017 Elsevier Inc. All rights reserved.

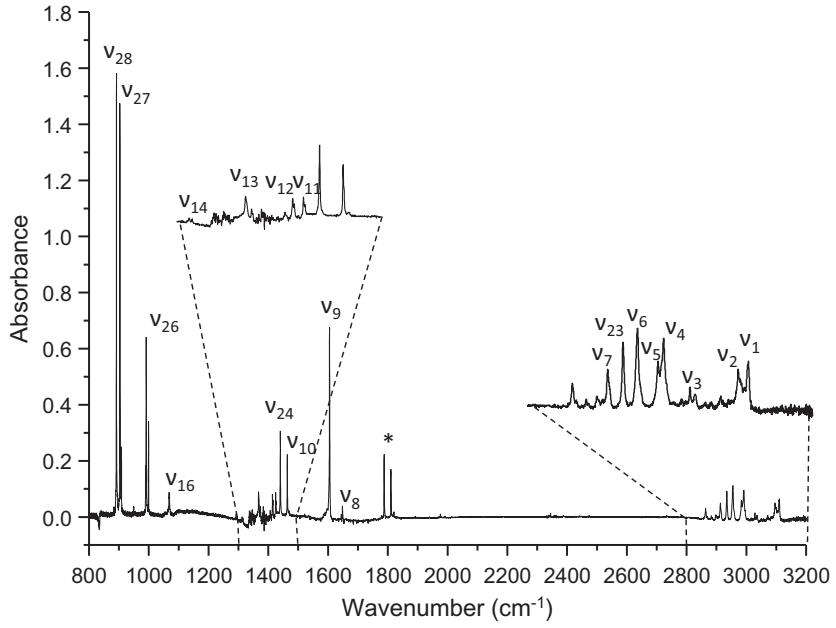


**Fig. 1.** Infrared spectrum of 2-methyl-1,3-butadiene (isoprene) recorded in the Ar matrix. Two insets show magnified views of C—H bending and C—H stretching regions, respectively, which are obscured in gas-phase spectra at room temperature. The asterisk corresponds to overtone or combination bands in the 1700–1900 $cm^{-1}$ region. Assignments of fundamental bands are based on Ref. [10] and the comparison with theoretical calculations in this study.

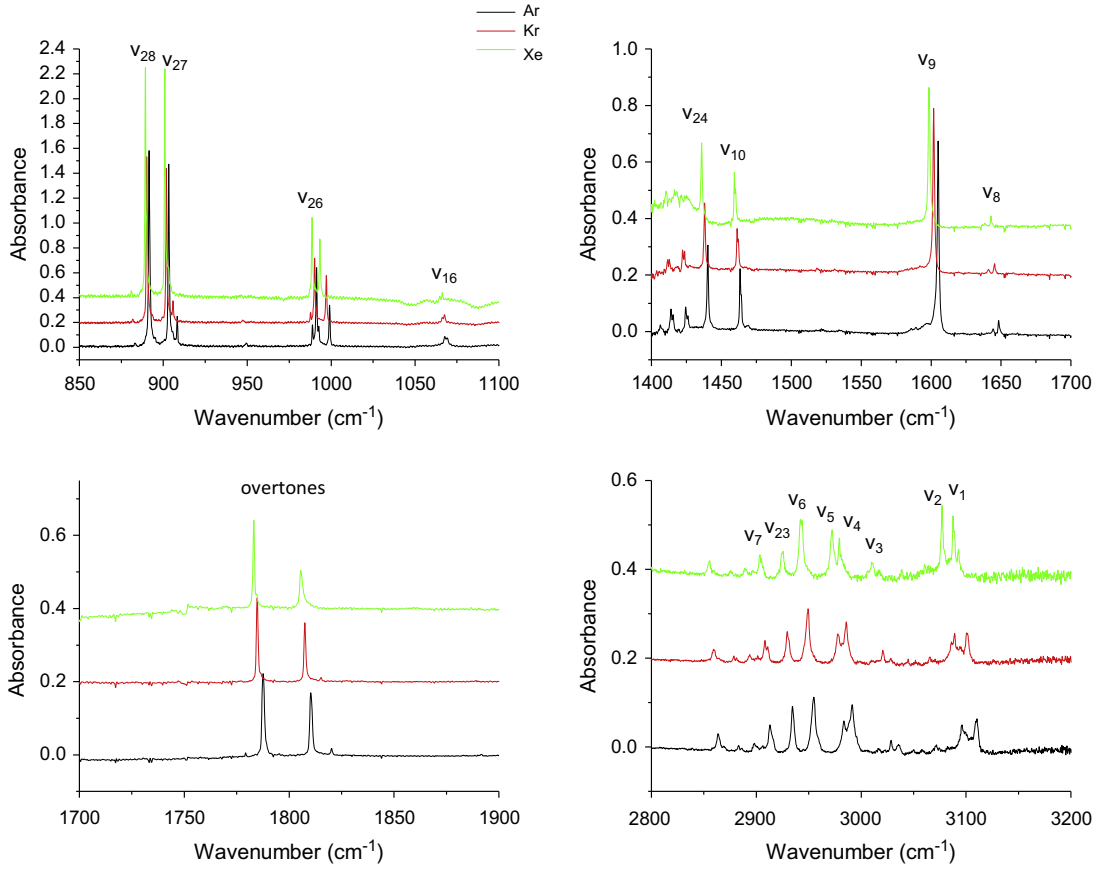


**Fig. 2.** Infrared spectra of isoprene in noble gas matrices. Assignments of fundamental bands are based on Ref. [10] and the comparison with theoretical calculations in this study. For the two bands in the 1750–1850 $cm^{-1}$ region, there exist several candidates including $\nu_{19} + \nu_{18}$, $\nu_{19} + \nu_{17}$ and so on.

and Xe. The IR spectrum of isoprene in the Xe matrix suffered from a low signal-to-noise ratio at around 1400 $cm^{-1}$, owing to the interplay of absorption and scattering of the condensed sample (the so-called Christiansen effect [22]); weak absorption peaks were not detected. The sequential red-shift of each vibrational peak from the Ar to Xe matrix reflects the increase in the host–

guest interaction, as has been reported previously [14,15,20]. Nevertheless, the overall vibrational structure remains unchanged in these three matrices, and the matrix shift caused by Xe is much smaller than that of the formic acid monomer in the corresponding vibrational region [15]. Hence, the interaction between isoprene and a noble gas atom is sufficiently weak for assigning its vibrational bands.

For the assignment of the satellite peaks observed at 908.3 and 999.0 $cm^{-1}$, the dependence of the spectra on the deposition temperature and sample concentration was investigated. As can be observed in Fig. 3, both satellite peaks, which are marked with downward arrows, exhibited a notable increase at high temperature and high concentration; hence, it is reasonable to conclude that the satellite peaks originate from polymeric species. Other satellite peaks were attributed to overtone or combination bands, because they did not exhibit any dependence on the temperature and sample concentration. The doublet structures observed for $\nu_{16}$, $\nu_{12}$, and $\nu_{11}$ bands were interpreted as "matrix effects." In contrast, other band peaks do not show any bifurcation, possibly due to the smaller splitting.

The relevance of these satellites to the assignments of weak fundamental bands ($\nu_{17}$, and $\nu_{25}$) has been discussed in a subsequent section.

Table 1 summarizes the peak positions of each vibrational band obtained by fitting to a Gaussian profile, together with calculated anharmonic frequencies.

## 3. Calculations

All calculations were performed using the GAUSSIAN 09 [23] package. The combination of the Becke–Lee–Yang–Parr functional (B3LYP) [24,25] and three basis sets, 6-31G(d,p), 6-31+G(2d,2p), and 6-311++G(3df,3pd), were used for the structure-optimization calculations of the most stable s-trans conformer. At the converged geometry, vibrational harmonic frequency calculations were performed to confirm that an energy minimum had been attained. Then, anharmonic vibrational frequencies were computed on the basis of a second-order perturbation theory [13,26] (VPT2). Table 2 summarizes the results obtained from these calculations.

From Table 2, it is clear that the harmonic wavenumbers ($\omega_{harm}$) were not dependent on the basis sets, and that the anharmonic corrections $\Delta\omega \equiv \omega_{anh} - \omega_{harm}$ were only within a few percent of $\omega_{harm}$. The $\Delta\omega$ obtained was negative, except for the two skeletal deformation vibrations $\nu_{21}$ and $\nu_{22}$ On the other hand, the calculated IR intensity (I) of each band was significantly dependent on the basis set. A factor of two variation in the intensities of six fundamental bands ($\nu_5$, $\nu_{15}$, $\nu_{20}$, $\nu_{25}$, $\nu_{30}$, and $\nu_{33}$) was observed from the 6-31G(d,p) to 6-311++G(3df,3pd) basis sets, and two fundamental bands ($\nu_{15}$ and $\nu_{33}$) exhibited significantly large discrepancies (ca. 8 and greater than 22, respectively). Such dependence can be explained by the subtle charge balance in isoprene: As C and H atoms have comparable electronegativity, the calculated charge distribution is dependent on the level of theory. Fig. 4 shows the Mulliken charge distribution in isoprene obtained at two levels of calculations: B3LYP/6-31G(d,p) and B3LYP/6-311++G(3df,3pd). Box arrows indicate the bond dipole moments of the corresponding C—H bonds. Notably, the charge distributions of the two central carbon atoms (C2 and C3) were different in the two sets of calculations, and this difference reflected the reversal of the bond moment, μ(C3—H6). As shown in Fig. 5, the two normal modes ($\nu_{15}$ and $\nu_{33}$) were attributed to the two C—H bonds, C3—H6 and C4—H7, and the change of the two bond moments, especially the reversal of μ(C3—H6), resulted in the variation of the transition moment, and hence the IR intensity of each band. Thus, it is imperative to achieve reproducibility for both band intensity and band position in order to assign fundamental bands for performing a comparison with theoretical calculations.

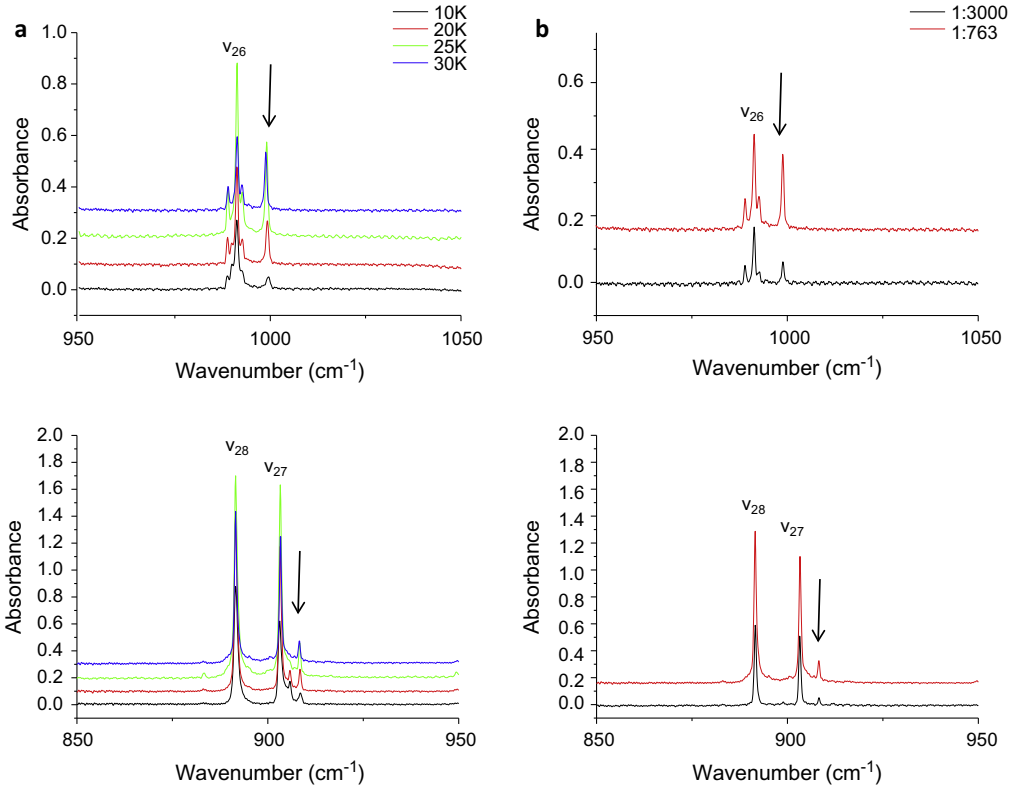


**Fig. 3.** Weak satellite bands near $\nu_{27}$ and $\nu_{26}$ bands in Ar are marked with arrows and their dependence on deposition temperature and sample concentration are shown.

**Table 1**
Observed peak positions of isoprene (in $cm^{-1}$) and vibrational assignments.

| Modes | Obs. | | | | Calc.[b,c] | |
|---|---|---|---|---|---|---|
| | Gas[a] | Ar[b] | Kr[b] | Xe[b] | B3LYP/6-31G(d,p) | B3LYP/6-311++G(3df,3pd) |
| $\nu_1$(A′) | 3101 | 3110.5 | 3100.8 | 3087.7 | 3105.7 | 3088.5 |
| $\nu_2$ | 3091 | 3096.2 | 3088.7 | 3076.9 | 3097.1 | 3081.3 |
| $\nu_3$ | 3017 | 3028.3 | 2977.9 | 2979.2 | 3026.6 | 3009.4 |
| $\nu_4$ | | 2991.1 | 2948.8 | 2972.2 | 3012.4 | 2987.8 |
| $\nu_5$ | | 2983.8 | 2929.7 | 2942.9 | 3001.4 | 2983.6 |
| $\nu_6$ | | 2054.5 | 2910.7 | 2925.0 | 2990.2 | 2970.2 |
| $\nu_7$ | | 2913.3 | 2893.5 | 2903.1 | 2917.8 | 2945.5 |
| $\nu_8$ | | 1644.2 | 1640.9 | 1642.7 | 1675.0 | 1652.0 |
| | | 1648.3 | 1645.2 | | | |
| $\nu_9$ | 1604 | 1604.9 | 1601.8 | 1598.5 | 1640.1 | 1617.1 |
| $\nu_{10}$ | 1467 | 1463.5 | 1461.3 | 1459.3 | 1477.8 | 1493.3 |
| | | | 1462.2 | 1460.1 | | |
| $\nu_{11}$ | 1428 | 1424.6 | 1422.2 | | 1434.4 | 1428.9 |
| | | 1426.4 | 1423.7 | | | |
| $\nu_{12}$ | 1417 | 1414.1 | 1411.6 | | 1421.6 | 1385.6 |
| | | 1415.7 | 1412.8 | | | |
| $\nu_{13}$ | 1384 | 1367.9 | 1365.2 | | 1386.0 | 1379.5 |
| $\nu_{14}$ | 1303 | 1312.2 | 1310.3 | | 1319.5 | 1294.1 |
| | | 1315.0 | 1312.8 | | | |
| $\nu_{15}$[d] | | | | | 1313.1 | 1305.6 |
| $\nu_{16}$ | 1071 | 1067.5 | 1066.4 | | 1079.1 | 1074.1 |
| | | 1069.4 | 1067.5 | | | |
| $\nu_{17}$[d] | | | | | 1002.7 | 1000.6 |
| $\nu_{18}$[d] | | | | | 952.7 | 945.1 |
| $\nu_{19}$ | | | | | 771.6 | 772.5 |
| $\nu_{20}$ | | | | | 530.0 | 531.7 |
| $\nu_{21}$ | | | | | 432.3 | 434.5 |
| $\nu_{22}$ | | | | | 282.1 | 282.0 |
| $\nu_{23}$(A″) | 2985 | 2934.5 | 2908.3 | 2904.8 | 2951.1 | 2932.7 |
| $\nu_{24}$ | 1444 | 1440.2 | 1437.9 | 1435.8 | 1465.1 | 1450.5 |
| $\nu_{25}$[d] | | | | | 1051.6 | 1045.7 |
| $\nu_{26}$ | 992 | 991.3 | 990.1 | 988.6 | 1009.7 | 1006.3 |
| | | 988.9 | 987.7 | | | |
| $\nu_{27}$ | 906 | 903.2 | 901.8 | 901.0 | 914.6 | 925.5 |
| $\nu_{28}$ | 894 | 891.6 | 890.2 | 889.4 | 904.1 | 912.6 |
| $\nu_{29}$ | 758 | | | | 771.3 | 769.3 |
| $\nu_{30}$ | | | | | 634.4 | 635.4 |
| $\nu_{31}$ | | | | | 398.5 | 407.2 |
| $\nu_{32}$ | | | | | 195.8 | 188.9 |
| $\nu_{33}$ | | | | | 156.4 | 156.8 |
| Overtones[e] | | 1787.6 | 1784.7 | 1783.2 | | |
| | | 1810.4 | 1807.4 | 1805.7 | | |
| | | 2863.6 | 2859.3 | 2855.1 | | |
| | | 2882.8 | 2878.6, | 2875.0 | | |
| | | 2898.4 | 2881.8 | 2889.8 | | |
| | | 3035.2 | 2985.5 | 3010.1 | | |
| | | | 3020.6 | | | |

[a] Ref. [10].
[b] This study.
[c] Anharmonic vibrational wavenumbers obtained in this study.
[d] Too weak to be observed. See text for the detailed assignments of these bands.
[e] There exist several candidates for these overtone/combination bands.

## 4. Results and discussion

Fig. 6 shows the comparison of the observed spectra of isoprene in the Ar matrix and the corresponding results obtained from anharmonic calculations. Gas-phase spectra recorded at room temperature are also shown. The most plausible assignments are indicated by broken lines, which connect the observed peaks and calculations. Quantitative agreement between the experimental and theoretical peak positions was observed in these regions. Unassigned peaks in the C—H stretching region (shown with asterisks) were attributed to overtone or combination bands that borrow intensity from fundamental bands.

Brauer et al. have reported the assignment of very weak bands, $\nu_{17}$ and $\nu_{25}$, in the gas-phase spectra [10], which were located in the Q-branch region of the $\nu_{26}$ and $\nu_{16}$ bands, respectively, as compared to the theoretical calculations reported by Panchenko et al. [9]. It was crucial to determine which band in our matrix spectra corresponds to each of these weak fundamentals for the complete assignment of fundamental bands in the observed region. As can be observed in Fig. 3, the $\nu_{26}$ band in the Ar matrix exhibited two satellite peaks at 988.9 and 999.0 $cm^{-1}$. The peak at 999.0 $cm^{-1}$ has already been assigned to the polymeric species. Assuming that the peak at 988.9 $cm^{-1}$ corresponds to $\nu_{17}$, the intensity ratio of this band to the strongest $\nu_{28}$ band, i.e., $I(\nu_{17})/I(\nu_{28})$, is calculated as 0.094, which is more than ten times greater than the theoretical estimate (0.21/41 = 0.0051, Table 2). Similarly, the assignment of one of the doublets of the $\nu_{16}$ band to the $\nu_{25}$ band is unlikely, because of the large discrepancy between the experimental intensity ratio ($I(\nu_{25})/I(\nu_{28})$ = 0.17) and its theoretical estimate ($I(\nu_{25})/I(\nu_{28})$ = 0.064/41 = 0.0016 from Table 2). Fig. 7 summarizes the relative intensities of the fundamental bands in the 900–1100 $cm^{-1}$ region, as determined from experimental peak areas and theoreti-

**Table 2**
Results of vibrational calculations for isoprene.

| Modes | B3LYP/6-31G(d,p) | | | B3LYP/6-31+G(2d,2p) | | | B3LYP/6-311++G(3df,3pd) | | |
|---|---|---|---|---|---|---|---|---|---|
| | $\omega_{harm}$[a] | $\omega_{anh}$[b] | I[c] | $\omega_{harm}$[a] | $\omega_{anh}$[b] | I[c] | $\omega_{harm}$[a] | $\omega_{anh}$[b] | I[c] |
| $\nu_1$(A′) | 3247.8 | 3105.7 | 17 | 3239.3 | 3095.3 | 14 | 3228.1 | 3088.5 | 12 |
| $\nu_2$ | 3240.0 | 3097.1 | 14 | 3230.6 | 3086.4 | 13 | 3220.7 | 3081.3 | 11 |
| $\nu_3$ | 3166.2 | 3026.6 | 3.5 | 3156.8 | 3022.5 | 3.2 | 3148.6 | 3009.4 | 2.8 |
| $\nu_4$ | 3155.5 | 3012.4 | 12 | 3145.8 | 2990.5 | 17 | 3139.2 | 2987.8 | 14 |
| $\nu_5$ | 3148.8 | 3001.4 | 10 | 3141.7 | 3003.7 | 3.6 | 3134.8 | 2983.6 | 4.0 |
| $\nu_6$ | 3133.1 | 2990.2 | 18 | 3119.5 | 2972.0 | 18 | 3112.1 | 2970.2 | 17 |
| $\nu_7$ | 3038.2 | 2917.8 | 19 | 3027.9 | 2935.8 | 22 | 3024.6 | 2945.5 | 20 |
| $\nu_8$ | 1719.7 | 1675.0 | 1.8 | 1694.9 | 1653.5 | 2.9 | 1693.5 | 1652.0 | 2.8 |
| $\nu_9$ | 1679.7 | 1640.1 | 18 | 1655.2 | 1617.2 | 32 | 1655.7 | 1617.1 | 33 |
| $\nu_{10}$ | 1515.8 | 1477.8 | 5.6 | 1501.3 | 1483.0 | 6.9 | 1502.9 | 1493.3 | 6.6 |
| $\nu_{11}$ | 1471.8 | 1434.4 | 1.3 | 1460.2 | 1423.7 | 2.0 | 1462.4 | 1428.9 | 2.5 |
| $\nu_{12}$ | 1442.9 | 1421.6 | 2.0 | 1431.6 | 1383.4 | 1.1 | 1432.5 | 1385.6 | 1.3 |
| $\nu_{13}$ | 1422.3 | 1386.1 | 4.3 | 1409.0 | 1374.2 | 5.1 | 1413.2 | 1379.5 | 5.8 |
| $\nu_{14}$ | 1338.5 | 1319.5 | 1.4 | 1329.6 | 1290.5 | 1.6 | 1331.5 | 1294.1 | 1.5 |
| $\nu_{15}$ | 1332.7 | 1313.1 | 0.12 | 1326.2 | 1299.0 | 0.12 | 1329.6 | 1305.6 | 0.015 |
| $\nu_{16}$ | 1094.7 | 1079.1 | 4.3 | 1088.6 | 1072.5 | 3.2 | 1091.9 | 1074.1 | 3.0 |
| $\nu_{17}$ | 1014.9 | 1002.7 | 0.20 | 1010.4 | 996.0 | 0.21 | 1014.5 | 1000.6 | 0.21 |
| $\nu_{18}$ | 967.4 | 952.7 | 0.63 | 962.3 | 945.3 | 1.1 | 961.7 | 945.1 | 1.1 |
| $\nu_{19}$ | 796.5 | 771.6 | 0.12 | 792.4 | 772.2 | 0.18 | 792.1 | 772.5 | 0.17 |
| $\nu_{20}$ | 535.7 | 530.0 | 0.14 | 535.0 | 527.9 | 0.067 | 538.5 | 531.7 | 0.044 |
| $\nu_{21}$ | 426.3 | 432.3 | 1.6 | 425.2 | 429.9 | 1.6 | 429.2 | 434.5 | 1.6 |
| $\nu_{22}$ | 280.1 | 282.1 | 0.91 | 278.2 | 279.0 | 1.0 | 280.7 | 282.0 | 0.98 |
| $\nu_{23}$(A″) | 3092.0 | 2951.1 | 21 | 3078.8 | 2934.9 | 15 | 3071.0 | 2932.7 | 14 |
| $\nu_{24}$ | 1493.5 | 1465.1 | 6.4 | 1480.8 | 1448.3 | 8.1 | 1482.4 | 1450.5 | 8.3 |
| $\nu_{25}$ | 1076.1 | 1051.6 | 0.22 | 1066.6 | 1042.0 | 0.19 | 1071.2 | 1045.7 | 0.064 |
| $\nu_{26}$ | 1033.9 | 1009.7 | 14 | 1028.2 | 1002.8 | 17 | 1032.4 | 1006.3 | 15 |
| $\nu_{27}$ | 930.3 | 914.6 | 21 | 930.9 | 914.2 | 35 | 943.2 | 925.5 | 41 |
| $\nu_{28}$ | 923.0 | 904.1 | 53 | 922.1 | 902.3 | 51 | 931.6 | 912.6 | 41 |
| $\nu_{29}$ | 789.3 | 771.3 | 0.39 | 784.0 | 766.1 | 0.49 | 788.6 | 769.3 | 0.51 |
| $\nu_{30}$ | 644.9 | 634.4 | 0.016 | 643.1 | 632.7 | 0.050 | 646.9 | 635.4 | 0.050 |
| $\nu_{31}$ | 407.9 | 398.5 | 5.5 | 410.9 | 405.1 | 11 | 412.0 | 407.2 | 10 |
| $\nu_{32}$ | 204.9 | 195.8 | 0.41 | 203.6 | 188.6 | 0.38 | 202.0 | 188.9 | 0.38 |
| $\nu_{33}$ | 163.6 | 156.4 | 0.0085 | 161.7 | 153.6 | 0.19 | 161.8 | 156.8 | 0.12 |

[a] Harmonic wavenumber in $cm^{-1}$.
[b] Anharmonic wavenumber in $cm^{-1}$.
[c] Infrared intensity in km $mol^{-1}$.

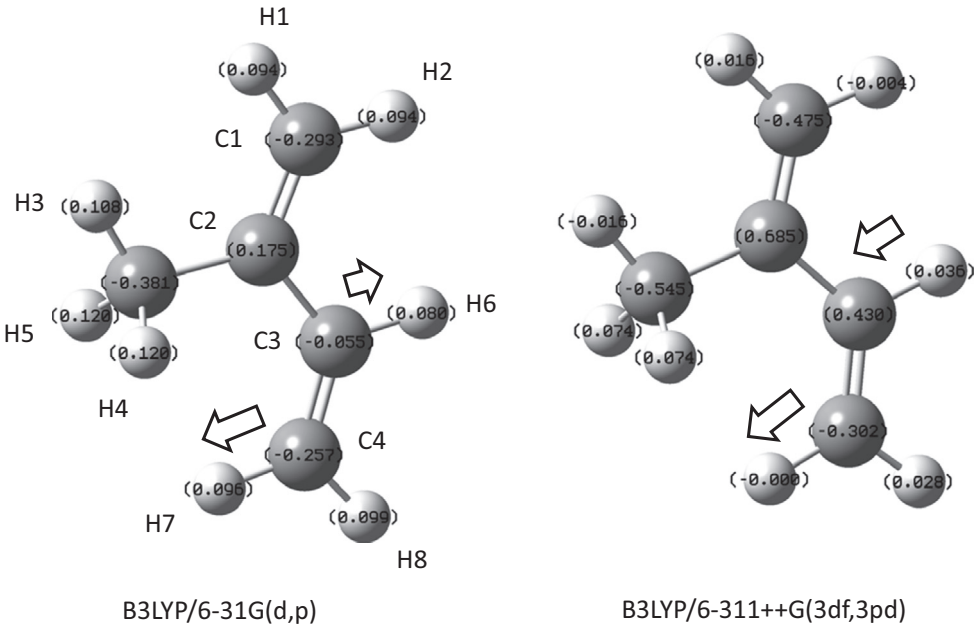


**Fig. 4.** Mulliken charge distribution of isoprene obtained at two levels of calculations, B3LYP/6-31G(d,p) and B3LYP/6-311++G(3df,3pd). Box arrows indicate bond moments of the C3-H6 and C4-H7 bonds. Notably, μ(C3—H6) is aligned in the opposite direction in the two calculations, owing to the drastic change in the charge of C3. See the main text for details.

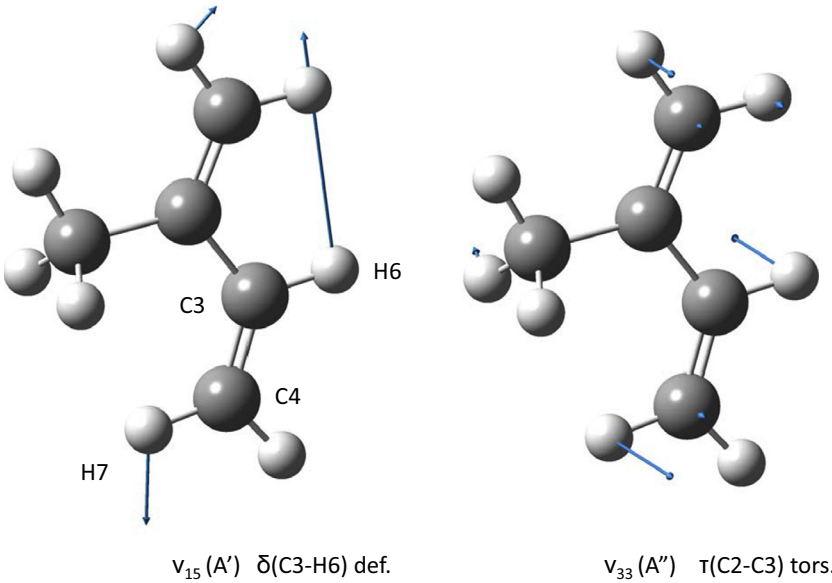


**Fig. 5.** Normal coordinates for the two fundamental bands $\nu_{15}$ and $\nu_{33}$. The approximate mode descriptions for the two bands are taken from Ref. [10]. Notably, $\nu_{15}$ (C3—H6 deformation) mainly corresponds to the in-plane bending of the C3—H6 bond, while $\nu_{33}$ (C2—C3 torsion) consists of the asynchronous out-of-plane bending of the C3—H6 and C4—H6 bonds.

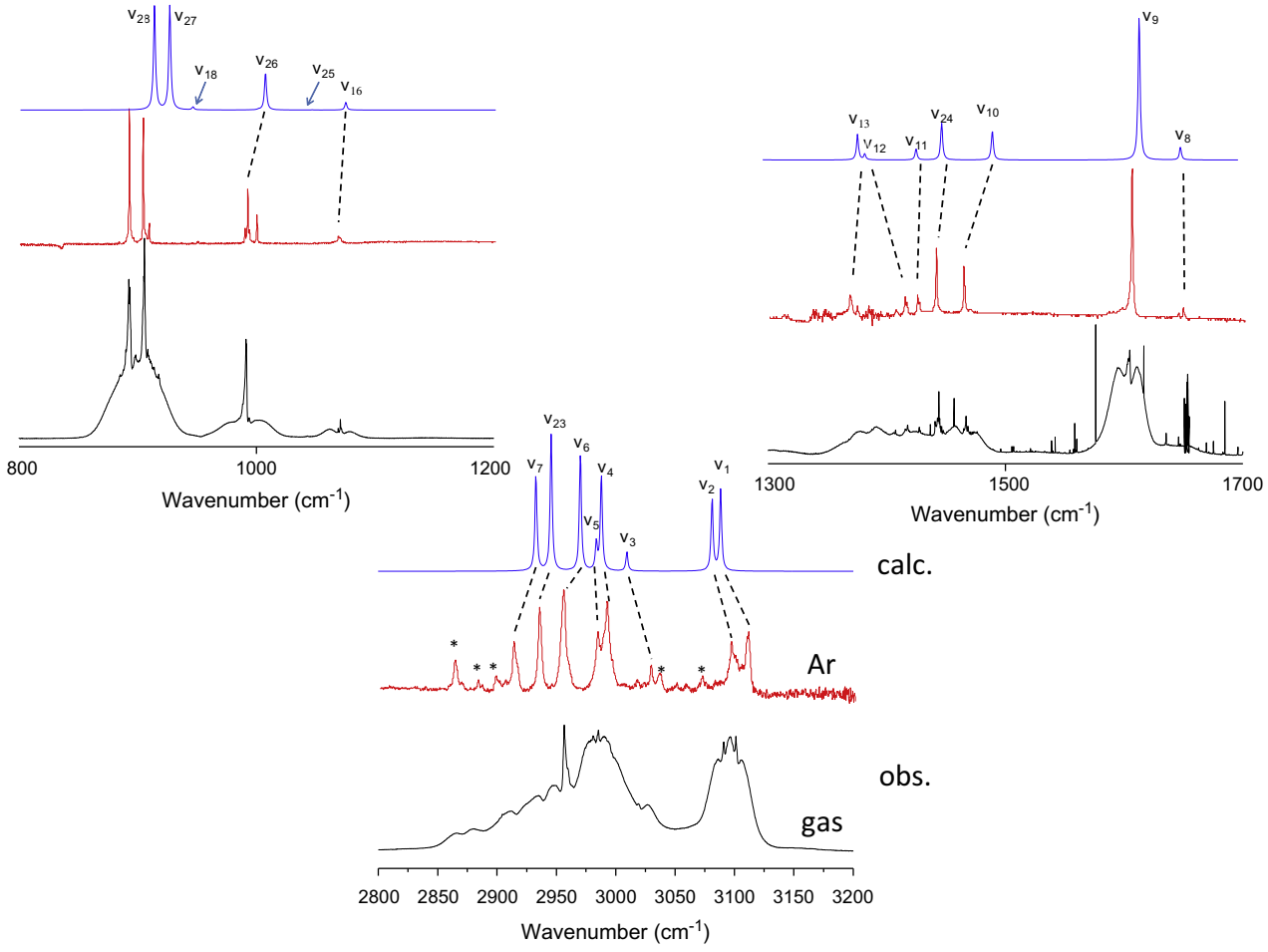


**Fig. 6.** A Comparison of the observed vibrational peaks with simulated spectra obtained from anharmonic calculations at the B3LYP/6-311++G(3df,3pd) level. The bottom trace shows a gas-phase spectrum recorded at room temperature.

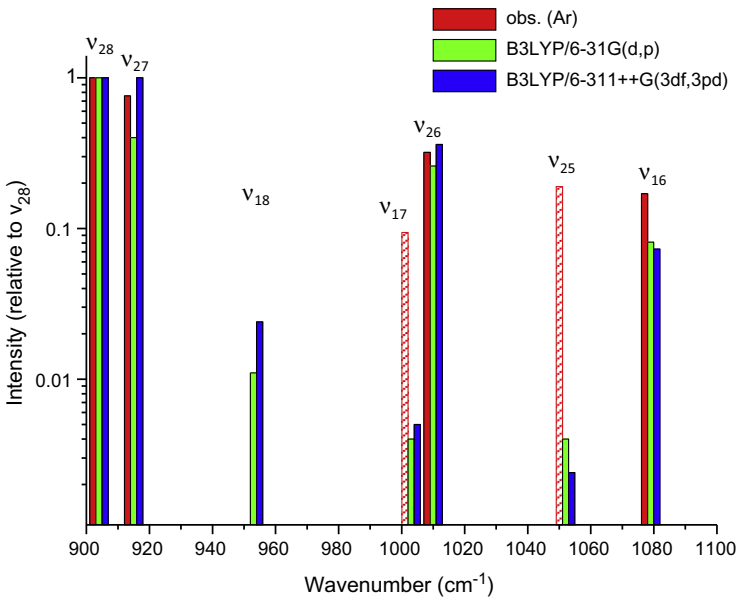


**Fig. 7.** A Stick diagram of the intensity pattern of fundamental bands in the 900–1100 $cm^{-1}$ region. The intensity of each band is normalized by that of the strongest band $\nu_{28}$. Notably, significant discrepancies are observed between the experimental and theoretical values for the weak bands $\nu_{17}$ and $\nu_{25}$, assuming that the weak satellites at 988.9 and 1069.4 $cm^{-1}$ corresponds to $\nu_{17}$ and $\nu_{25}$, respectively. The entry for the experimental band intensity for $\nu_{18}$ is kept blank due to the unsuccessful identification of this band.

cal calculations. Strong bands clearly exhibited an intensity pattern comparable to calculations, whereas none of these satellite bands were attributable to the weak fundamental bands. On the other hand, we could not find any vibrational peak that is assignable to $\nu_{18}$ in this region, similarly to Ref. [10].

Hence, it is reasonable to conclude that the two fundamental bands ($\nu_{17}$ and $\nu_{25}$) are too weak to be observed and that the bands reported by Brauer et al. [10] are, in reality, hot bands of $\nu_{26}$ and $\nu_{16}$, as isoprene exhibits three low-frequency modes ($\nu_{22}$, $\nu_{32}$, and $\nu_{33}$), which are well populated even at room temperature.

## 5. Conclusion

In this study, the infrared (IR) spectra of isoprene in noble gas matrices were reported for the first time. Peak positions of fundamental bands were compared to anharmonic vibrational frequencies obtained from density functional theory calculations. We presented alternative assignments of weak bands ($\nu_{17}$ and $\nu_{25}$) of gas-phase spectra at room temperature. The influence of hot bands in the spectra of isoprene would require re-evaluation of infrared absorption cross sections of other bands that have been used in-situ monitoring of this species. To confirm these assignments, high-resolution observations of relevant bands of isoprene in gas phase, with varying temperature, would be required.

## References

[1] F. Paulot, J.D. Crounse, H.G. Kjaergaard, A. Kürten, J.M. St. Clair, J.H. Seinfeld, P. O. Wennberg, Science 325 (2009) 730–733.
[2] D.R. Worton, J.D. Surratt, B.W. LaFranchi, A.W.H. Chan, Y. Zhao, R.J. Weber, J.-H. Park, J.B. Gilman, J. de Gouw, C. Park, G. Schade, M. Beaver, J.M. St. Clair, J. Crounse, P. Wennberg, G.M. Wolfe, S. Harrold, J.A. Thornton, D.K. Farmer, K.S. Docherty, M.J. Cubison, J.-L. Jimenez, A.A. Frossard, L.M. Russell, K. Kristensen, M. Glasius, J. Mao, X. Ren, W. Brune, E.C. Browne, S.E. Pusede, R.C. Cohen, S.H. Seinfeld, A.H. Goldstein, Environ. Sci. Technol. 47 (2013) 11403–11413.
[3] F. Kühnemann, M. Wolfertz, S. Arnold, M. Lagemann, A. Popp, G. Schüler, A. Jux, W. Boland, Appl. Phys. B 75 (2002) 397–403.
[4] D.R. Lide Jr., M. Jen, J. Chem. Phys. 40 (1964) 252–253.
[5] D.A.C. Compton, W.O. George, W.F. Maddams, J. Chem. Soc. Perk. T 2 (1976) 1666–1671.
[6] M. Traetteberg, G. Paulen, S.J. Cyvin, Y.N. Panchenko, V.I. Mochalov, J. Mol. Struct. 116 (1984) 141–151.
[7] C.W. Bock, Y.N. Panchenko, S.V. Krasnoshchiokov, J. Mol. Struct. 160 (1987) 337–346.
[8] C.W. Bock, Y.N. Panchenko, J. Mol. Struct. 187 (1989) 69–82.
[9] Y.N. Panchenko, C.W. Bock, J.D. Larkin, A.V. Abramenkov, F. Kühnemann, Struct. Chem. 19 (2008) 421–428.
[10] C.S. Brauer, T.A. Blake, A.B. Guenther, S.W. Sharpe, R.L. Sams, T.J. Johnson, Atmos. Meas. Tech. 7 (2014) 3839–3847.
[11] Y.N. Panchenko, A.V. Abramenkov, C.W. Bock, J. Mol. Struct. 140 (1986) 87–92.
[12] P. Sahay, S.T. Scherrer, C. Wang, Sensors 13 (2013) 8170–8187.
[13] V. Barone, J. Chem. Phys. 122 (2005) 014108.
[14] F. Ito, J. Mol. Struct. 1118 (2016) 161–166.
[15] F. Ito, J. Mol. Struct. 1091 (2015) 203–209.
[16] F. Ito, J. Mol. Struct. 1035 (2013) 54–60.
[17] F. Ito, J. Chem. Phys. 137 (2012) 014505.
[18] F. Ito, J. Mol. Struct. 1012 (2012) 43–49.
[19] F. Ito, Chem. Phys. 382 (2011) 52–57.
[20] F. Ito, Chem. Phys. 369 (2010) 82–90.
[21] G. Herzberg, Infrared and Raman Spectra of Polyatomic Molecules, Van Nostrand Reinhold, 1945. p. 271.
[22] See, for example H.R. Carlon, Appl. Opt. 18 (1979) 3610–3614.
[23] M.J. Frisch, G.W. Trucks, H.B. Schlegel, G.E. Scuseria, M.A. Robb, J.R. Cheeseman, G. Scalmani, V. Barone, B. Mennucci, G.A. Petersson, H. Nakatsuji, M. Caricato, X. Li, H.P. Hratchian, A.F. Izmaylov, J. Bloino, G. Zheng, J.L. Sonnenberg, M. Hada, M. Ehara, K. Toyota, R. Fukuda, J. Hasegawa, M. Ishida, T. Nakajima, Y. Honda, O. Kitao, H. Nakai, T. Vreven, J.A. Montgomery, Jr., J.E. Peralta, F. Ogliaro, M. Bearpark, J.J. Heyd, E. Brothers, K.N. Kudin, V.N. Staroverov, R. Kobayashi, J. Normand, K. Raghavachari, A. Rendell, J.C. Burant, S.S. Iyengar, J. Tomasi, M. Cossi, N. Rega, J.M. Millam, M. Klene, J.E. Knox, J.B. Cross, V. Bakken, C. Adamo, J. Jaramillo, R. Gomperts, R.E. Stratmann, O. Yazyev, A.J. Austin, R. Cammi, C. Pomelli, J.W. Ochterski, R.L. Martin, K. Morokuma, V.G. Zakrzewski, G.A. Voth, P. Salvador, J.J. Dannenberg, S. Dapprich, A.D. Daniels, Ö. Farkas, J.B. Foresman, J.V. Ortiz, J. Cioslowski, D.J. Fox, Gaussian 09, Revision A.2, Gaussian Inc., Wallingford, CT, 2009.
[24] P.J. Stephens, F.J. Devlin, C.F. Chabalowski, M.J. Frisch, J. Phys. Chem. 98 (1994) 11623–11627.
[25] R.H. Hertwig, W. Koch, Chem. Phys. Lett. 268 (1997) 345–351.
[26] V. Barone, J. Bloino, C.A. Guido, F. Lipparini, Chem. Phys. Lett. 496 (2010) 157–161.